14

Isotopic Constraints on the Formation of the Main Belt

KATHERINE R. BERMINGHAM AND THOMAS S. KRUIJER

14.1 INTRODUCTION

Nucleosynthetic and radiogenic isotope data from meteorites have enabled significant advancements to be made in understanding how the protoplanetary disk evolved into the Solar System. A potentially strict isotopic divide between the inner and outer protoplanetary disk has been inferred using data from some of the earliest formed asteroids. This isotope dichotomy has been interpreted to indicate that early Jupiter formation divided the protoplanetary disk, which significantly influenced the type of material available for terrestrial planet formation. These findings are discussed in this chapter, with an emphasis on Vesta and Ceres as these asteroids likely originated from the inner and outer disk, respectively.

As remnants of planet formation, meteorites provide the most direct samples of the protoplanetary disk. These cosmochemical materials are analyzed in detail to produce a wealth of chemical, isotopic, and petrographic data which provide some of the most stringent constraints on the composition of the disk. Synthesizing this information with constraints from astronomical observations, astrophysical models, disk dynamics, and planetary accretion models contextualizes the compositional data and generates a picture of Solar System and planet formation.

Particularly valuable sample-based data are mass-independent nucleosynthetic isotope compositions of bulk meteorites. Here, "bulk meteorite" refers to a whole rock sample of a meteorite, in contrast to meteorite components[1] or mineral separates which are isolated minerals from a bulk meteorite. The range of nucleosynthetic isotope compositions recorded by meteorites stems from parent bodies incorporating different proportions of presolar grains. Over the past 15 years, datasets of nucleosynthetic isotope variations[2] in meteorites have greatly expanded (for a review see Qin & Carlson, 2016). The magnitude and nature of nucleosynthetic isotope variations are now commonly used to infer the "building blocks" or stellar precursors of the Solar System, the dynamical processes that controlled their distribution in the protoplanetary disk and, potentially, the compositional structure of the disk itself.

Based on the nucleosynthetic isotope signatures of different meteorites, an apparently strict grouping was identified (Warren, 2011). Meteorites, and thus their parent bodies, fall into one of two groups: the noncarbonaceous chondrite group (NC) and the carbonaceous chondrite group (CC). The terminology was based on the predominance of unmelted carbonaceous chondrites in the CC group, whereas the NC group was devoid of these materials. The use of these terms to describe the isotope dichotomy is somewhat of a misnomer, because both groups include iron and stony-iron meteorites (e.g., Warren, 2011; Kruijer et al., 2017; Bermingham et al., 2018b) which are chemically and petrographically distinct from carbonaceous chondrites. The NC and CC terminology, however, is used to describe an isotopic classification that supersedes the traditional classification of meteroites into chondrite or achondrite groups as based on the composition, mineralogy, and texture of a sample. The NC–CC terminology has become convention in the literature and will be followed here.

In addition to information provided by nucleosynthetic isotope variations in meteorites, radiometric isotope signatures of meteorites and their components date Solar System and parent body processes (for a review see Kleine & Wadhwa, 2017). For example, the first condensates to form in the protoplanetary disk are CAIs, which have an average absolute U-corrected Pb–Pb age of 4,567.30 ± 0.16 Ma (e.g., Connelly et al., 2012). Calcium aluminum inclusions are small (μm to cm-sized) inclusions composed of refractory[3] element oxides. The 4,567.30 ± 0.16 Ma CAI age is generally taken to be the cosmochemical start of the Solar System (t_0) and all relative ages defined by radiometric systems are compared to this start time. Less than 1 Ma after t_0, accretion of planetesimals (whose radii range from tens to hundreds of kilometers) and differentiation began. The timescales of early accretion and differentiation of planetesimals are determined using short-lived radioactive isotope systematics and thermal modeling of meteorite parent body accretion (e.g., Kruijer et al., 2014, 2017; Sugiura & Fujiya, 2014; Desch et al., 2018; Hilton et al., 2019).

By comparing the nucleosynthetic isotope compositions of NC and CC meteorites with their accretion ages, parent body accretion locations in the disk and the timing of Jupiter's formation were

Our sincere thanks to the editors, S. Marchi, C. A. Raymond, and C. T. Russell, for their invitation to contribute to this edition and thorough reviews. We also thank E. R. D. Scott for his insightful review. K. R. B. was supported by NASA Emerging Worlds grant 80NSSC18K0496, NASA SSERVI grant NNA14AB07A, NASA Emerging Worlds grant NNX16AN07G, and the Department of Earth and Planetary Sciences, Rutgers University. T. S. K. was supported by the Laboratory Directed Research and Development Program at Lawrence Livermore National Laboratory (grant 20-ERD-001). This study was in part performed under the auspices of the US DOE by Lawrence Livermore National Laboratory under contract DE-AC52–07NA2734.

[1] Calcium aluminum inclusions (CAIs), ameboid olivine aggregates (AOAs), and chondrules (which are millimeter-sized igneous spherules).

[2] Isotope variations are defined as isotope ratios that are in excess or depletion relative to a terrestrial reference value, where terrestrial materials are generally defined as "normal" (or equal to zero) in isotopic composition.

[3] Refractory elements have 50% condensation temperatures above 1,335 K, moderately volatiles between 1,335 and 665 K, volatile elements below 665 K, and highly volatile elements below 371 K (for a gas of solar composition at a total pressure of 10^{-4} bar; Lodders, 2003).

https://doi.org/10.1017/9781108856324.018 Published online by Cambridge University Press

inferred (Kruijer et al., 2017). Noncarbonaceous chondrite parent bodies were suggested to originate from the inner disk and CC parent bodies from the outer disk (Warren, 2011; Kruijer et al., 2017), where inner disk refers to the region inbound of the heliocentric distance where Jupiter formed and outer disk refers to the outbound region from Jupiter. Warren (2011) and Kruijer et al. (2017) postulated that the inner and outer disk regions were separated by an early formed Jupiter which inhibited mixing material between the two regions until giant planets migration toward the end of the disk's lifetime (following Walsh et al., 2011).

This chapter discusses NC–CC isotope dichotomy and its role in advancing the reconstruction of early Solar System evolution. The chapter begins by reviewing Main Belt asteroids and meteorites. Following this is an introduction to presolar grains and how their heterogeneous distribution in the protoplanetary disk produced nucleosynthetic isotope variability, and the significance of radiometric dating. Then there is a discussion about how the NC–CC isotope dichotomy is defined, its proposed causes, and implications for protoplanetary disk evolution. The chapter concludes with a discussion about the history of Ceres and Vesta in the context of the NC–CC isotope dichotomy.

14.2 SOLAR SYSTEM ORIGINS AND EARLY EVOLUTION

The protoplanetary disk developed from a segment of the parental molecular cloud, composed of presolar gas and dust grains, which had spun into a disk around the nascent Sun. The cause of the separation of the segment from the parental molecular cloud remains debated, but a shockwave from a nearby supernova may have triggered the collapse, or it may have occurred because of a weakening of magnetic field support following ambipolar diffusion (Cameron & Truran, 1977; Shu et al., 1987). If a supernova triggered the collapse of the disk, it is a potential source of short-lived radioactive isotopes for the Solar System (e.g., Dauphas & Chaussidon, 2011). Alternatively, the Solar System may have been formed by a triggered star formation at the edge of a Wolf-Rayet bubble (Dwarkadas et al., 2017). A supernova trigger event, however, is not required as the observed abundances of short-lived radioactive isotopes may be what is expected in average star-forming clouds (Young, 2014). The original protoplanetary disk was a common by-product of the star forming process, where such disks typically range in mass from 0.001 to 0.3 Solar masses (10^{27}–10^{29} kg) and in size from 10^{12} to 10^{14} m (Hogerheijde, 2011). The protoplanetary disk comprised gas (∼99% by mass) and solids (∼1%). The gas was predominately H and He, with volatile compounds such as CO and H_2O also present. The dust grains included material from different stellar sources added to the interstellar medium at least 3 ± 2 Ga before the start of the Solar System (e.g., Heck et al., 2020).

Shortly after CAIs formed, small bodies began to rapidly accrete to form planetesimals, possibly aided by electrostatic and magnetic forces and the formation of pebbles (e.g., Blum & Wurm, 2000; Lambrechts & Johansen, 2012). Collisional accretion of planetesimals and subsequent oligarchic growth produced the observed planetary system. Planetary accretion and its relationship to the dynamical evolution of the protoplanetary disk are described in detail in Chapters 13 and 15.

14.3 THE MAIN ASTEROID BELT AND METEORITES

14.3.1 The Main Asteroid Belt

All known meteorites (∼40,000 specimens),[4] except those from Mars and the Moon, originate from the asteroid belt. Meteorites are estimated to come from ∼100 parent bodies (e.g., Delbo' et al., 2017; Dermott et al., 2018; Greenwood et al., 2020) and many meteorites have been linked to specific asteroid types (for a review see Vernazza & Beck, 2017; Chapter 1). The extent to which the main asteroid belt samples the protoplanetary disk, however, remains uncertain, and it is likely that much of the asteroid belt has not been sampled by meteorites that fall to Earth. Nevertheless, the mineralogical, textural, elemental, and isotopic studies of meteorites reveal significant compositional diversity in the protoplanetary disk. Moreover, as meteorites are among the only available hand samples of the protoplanetary disk, they provide the most robust constraints on the composition of planetary building blocks and planetary accretion.

The main asteroid belt houses >1,000,000 asteroids, but the total mass of the main asteroid belt is ∼0.05% of Earth's mass. Two of its largest bodies, Vesta and Ceres, account for ∼9% and ∼25% of the total mass of the asteroid belt, respectively. Presently, the asteroid belt is radially zoned, with S-type asteroids ("dry" asteroids) dominating the inner belt and C-type asteroids ("wet" asteroids) dominating the outer belt (Gradie & Tedesco, 1982; DeMeo & Carry, 2014; Chapter 1). Asteroid scattering caused by giant planet migration during the final stages of the disk's lifetime, however, likely disrupted the asteroid belt significantly (e.g., Walsh et al., 2011; Raymond & Izidoro, 2017b). Hence, the present distribution of asteroids in the Main Belt is unlikely to reflect their original accretion locations in the Solar System.

An example of the compositional diversity in the main asteroid belt is evident when comparing Vesta (V-type asteroid, 525 km diameter) and Ceres (C-type asteroid, 946 km in diameter). Vesta has been linked to howardite, eucrite, and diogenite (HED) meteorites (Binzel & Xu, 1993). Chapter 3 discusses this relationship using a synthesis of data collected during the Dawn mission and from HED meteorites. Carbonaceous chondrites have been linked to C-type asteroids, of which Ceres is an example (Burbine, 1998), but, unlike Vesta, there are no confirmed meteorite samples of Ceres.

Vesta and Ceres could not be more different in composition. Vesta is a differentiated rocky asteroid with a metallic core and silicate mantle and crust. This asteroid has a density of 3,456 kg/m^3 (Russell et al., 2012), is water- and organic-poor compared to Ceres, and may have accumulated hydrogen on the surface via the addition of carbonaceous chondrite material after accretion (Prettyman et al., 2012; Sarafian et al., 2014). By contrast, Ceres is the largest asteroid in the main asteroid belt but it has a lower density of 2,162 kg/m^3 (Russell et al., 2016; Konopliv et al., 2018) and a C-rich surface. Ceres is modeled to have 12–29 vol% of macromolecular organic matter and Ceres-forming materials may have been more water-rich than some of the most hydrated meteorites documented (e.g., CI chondrites; Prettyman et al., 2017; Marchi et al., 2019). Although gravity data of Ceres suggest a

[4] The meteorites discussed in this contribution do not include micrometeorites.

https://doi.org/10.1017/9781108856324.018 Published online by Cambridge University Press

two-layer structure with an abrupt density change, this body did not undergo igneous differentiation like Vesta (see Chapter 12 for a comparative discussion about the structure of Ceres and Vesta).

14.3.2 Meteorites and Their Components

Although meteorites fall into one of two petrographic types, melted or unmelted, they vary significantly in composition which reflects the diversity in asteroid types and the different parts of a asteroid sampled by meteorites. Melted meteorites (also known as achondrites or differentiated meteorites) originate from rocky asteroids that underwent wholescale melting and differentiation to form a parent body with a metallic core, and silicate mantle and crust (e.g., Vesta). The melting process of what would have begun as an undifferentiated asteroid was likely caused by the presence of short-lived radioactive isotopes which produced heat via the decay of an unstable parent to a stable daughter species (short-lived species have half-lives $(t_{1/2}) < 100$ Ma; Dauphas & Chaussidon, 2011). Efficient differentiation of asteroids only occurred for those larger than a minimum threshold and at the same time contained sufficient heat-producing radioactive isotopes (capable of producing high temperatures >1,773 K in some cases; Taylor et al., 1993). The short-lived radioactive isotope ^{26}Al ($^{26}\text{Al} \rightarrow {}^{26}\text{Mg}$, $t_{1/2} = 0.73$ Ma; Lee et al., 1977; Hevey & Sanders, 2006) is considered to be the primary heat-producing isotope that caused some parent bodies to undergo wholescale melting, where after ~3 Ma this heat source for melting rocky material was extinct (e.g., Elkins-Tanton, 2012). Tang and Dauphas (2012) concluded the current best estimate for the Solar System initial ^{60}Fe/^{56}Fe ratio $(1.0 \pm 0.3 \times 10^{-8})$ indicates heating from ^{60}Fe decay $(t_{1/2} \sim 2.6\,\text{Ma})$ would have been negligible and thus this ^{60}Fe did not significantly contribute to the heat required for planetesimal differentiation. Short-lived radioactive isotope systematics indicate that differentiation of a planetesimal to form a core (^{182}Hf–^{182}W; Kleine et al., 2009), mantle, and crust (^{53}Mn–^{53}Cr; Trinquier et al., 2008) occurred relatively quickly (<3 Ma). As outlined in Chapter 3, however, some meteorites from Vesta have had longer (>10 Ma) magmatic or cooling histories.

While achondrites sample a range of different parent bodies, they also sample distinct domains of individual asteroids. For instance, some achondrites are samples of the crust, mantle, or a mixture of these silicate layers. Of these, Vesta is the most well-sampled parent body, Vesta's mantle, crust, or a mixture of the two are identified in diogenites, eucrites, or howardites, respectively. Other achondrites, iron meteorites, are samples of the core or metal-dominated portion of an asteroid. Based on their compositions, iron meteorites were originally classified into 14 different chemical groups based on their trace element compositions, where ~15% are ungrouped (for review see Krot et al., 2014). Iron meteorites, however, have not yet been chemically or isotopically linked to known achondrites, which suggests that the silicate mantles of iron meteorite parent bodies are "missing," possibly destroyed by impacts in the early Solar System. Magmatic iron meteorites are FeNi alloys with ≤1 wt.% Co, S, P, and C (Buchwald, 1975; Scott & Wasson, 1976; Goldstein et al., 2009; Krot et al., 2014), and likely sample different stages of fractional crystallization of a core (Lovering, 1957; Scott, 1972). Non-magmatic iron meteorites have macroscopic silicates, graphite, and carbides, indicating a different history to magmatic iron meteorites. Unlike magmatic iron meteorites, the chemical composition of non-magmatic iron meteorites cannot be produced by simple fractionation crystallization of a core, but likely sample more complex, multi-stage metal–silicate segregation events on differentiated parent bodies (e.g., Scott, 1972; Benedix et al., 2000; Wasson & Kallemeyn, 2002; Worsham et al., 2016, 2017). Stony iron meteorites (mesosiderites or pallasites) contain mixtures of silicates, Fe-Ni metal, and troilite (for a review see Krot et al., 2014). Main group pallasites may represent the transition zone between the core and mantle of differentiated asteroids (Scott, 1977), however, updated metallographic cooling rates suggest an impact origin for these meteorites (Yang et al., 2007, 2010), possibly including an influx of core–metal from the impactor (Walte et al., 2020).

Unmelted meteorites, also known as chondrites or undifferentiated meteorites, come from asteroids that have not undergone wholescale melting. Chondrites are the most common undifferentiated meteorite type (for a review see Krot et al., 2014). Unlike melted meteorites, unmelted meteorites preserve a variety of disk-derived components that are held together by a matrix of fine-grained dust. Disk-derived components include CAI, chondrules, AOAs, and presolar grains (Krot et al., 2009; MacPherson, 2014). It is likely that both melted and unmelted meteorites accreted meteorite components, but the melting process which differentiated parent bodies altered the components beyond visual recognition. Volatile species can be more abundant in chondrites as compared to achondrites, although the volatile content varies significantly between different chondrite groups (for a recent review see Bermingham et al., 2020). Although there are no confirmed samples from Ceres, it is the largest object in the main asteroid belt and has been classified as a "wet" unmelted asteroid. The exact reason why Ceres remained undifferentiated may well be related to the absence of sufficient ^{26}Al to cause widespread melting of the parent body. Why Ceres might have lacked ^{26}Al is not yet clear, but it could be related to a relatively late accretion time (i.e., after extinction of ^{26}Al) and/or processes that internally redistributed ^{26}Al on Ceres (see Chapter 11 for more details).

14.3.3 Presolar Grains

As chondrites have not undergone wholescale melting, they preserve remnants of material that was present in the protoplanetary disk. In addition to meteorite components such as CAIs, chondrules, and AOAs, chondrites preserve small (≤μm-scale) presolar grains. Presolar grains are defined as "stardust that formed in stellar outflows or ejecta and remained intact throughout its journey into the solar system where it was preserved in meteorites" (Lodders & Amari, 2005, p. 94). Through laboratory studies of residues that remained after dissolving undifferentiated meteorites in concentrated oxidizing acid, part of the ~1% (by mass) of the protoplanetary disk's solid material inherited from the parental molecular cloud was identified. Through isotopic and structural analysis of the residual slurries and individual grains, these chemically robust solids were recognized as presolar in origin (Lewis et al., 1987; Zinner et al., 1987). Presolar materials are characterized by highly variable (~1 to 0.1%) isotopic compositions which develop by virtue of their formation in stellar environments (for a review see Zinner, 2014).

Lodders and Amari (2005) and Huss and McSween (2010) provide thorough reviews of presolar grains, their origins,

https://doi.org/10.1017/9781108856324.018 Published online by Cambridge University Press

composition, and significance in cosmochemistry. To summarize these reviews, there are two types of presolar grains: circumstellar condensates and interstellar grains. Circumstellar condensates are *bone fide* presolar grains. They condensed from hot gas ejected from dying stars in the immediate vicinity of their parent stars and remained intact until they were preserved in meteorites (Huss & McSween, 2010). The elemental and isotopic composition of these grains can be directly linked to their stellar source, and presolar grains have markedly different compositions to materials formed within the Solar System. Interstellar grains are distinct from circumstellar grains because they formed in interstellar space. These grains did not survive the long journey from their stars, rather they are vaporized circumstellar condensates which eventually recondensed into grains within molecular clouds. Interstellar grains often lack a mineral structure and have variable elemental and isotopic compositions which reflects their mixture of material from different stellar sources (Huss & McSween, 2010).

14.4 NUCLEOSYNTHETIC ISOTOPE ANOMALIES

A comparison between meteorites and terrestrial samples reveals isotopic variability in the following elements: Ca, Ti, Cr, Ni, Sr, Zr, Mo, Ru, Pd, Ba, W, Nd, Sm, HREE, and noble gases (Ne, Ar, Kr, Xe) (e.g., Warren, 2011; Ott, 2014; Mayer et al., 2015; Qin & Carlson, 2016; Bermingham et al., 2016, 2018a, 2018b; Dauphas & Schauble, 2016; Kruijer et al., 2017; Nanne et al., 2019). These isotope variations are independent of radiogenic decay, mass-dependent anomalies, cosmic ray exposure effects, and nuclear field shift effects, although some of these effects can overprint nucleosynthetic isotope compositions. Nucleosynthetic isotope compositions vary from terrestrial compositions by 10s to 1,000s of parts per million (ppm). The variations are reported in either epsilon (ε), which reflects the compositional deviation from a terrestrial standard in parts per 10,000, or mu (μ), the parts per 1000,000 deviation.

Nucleosynthetic isotope anomalies in bulk meteorites and planetary bodies arise as a consequence of the heterogeneous distribution of highly isotopically variable presolar grains in the protoplanetary disk. Nucleosynthetic isotope variations are similar to those seen in presolar grains, but they are of smaller magnitude (~0.001–0.01%). The heterogeneous distribution of presolar grains is thought to be the result of poor mixing of these grains into the protoplanetary disk (Clayton, 1982, and references therein) and/or their selective destruction via thermal chemical processing in the protoplanetary disk (Trinquier et al., 2009).

Bulk meteorite isotopic variations are generally considered to reflect the average composition of the parent body and thus the nebular region from which it accreted (e.g., Walker et al., 2015). Nucleosynthetic isotope variations are used to assess the "genetic" relationships between meteorites and their parent bodies, where the term "genetic" refers to the average isotopic compositions of the primary nebular materials from which an object was built (Walker et al., 2015).

The nucleosynthetic isotope composition of an unmelted parent body is determined by bulk rock lithophile and siderophile isotope measurements of a meteorite. In melted parent bodies, the bulk lithophile isotope composition is best represented by whole rock analyses of meteorites originating from the silicate portion of the body. Bulk parent body siderophile isotope compositions of melted bodies can most reliably be obtained by analyzing material that sample well-mixed siderophile element compositions, such as from the core (magmatic iron meteorites) or metal portions of large impact melt sheets (non-magmatic iron meteorites) (Worsham et al., 2016; Bermingham et al., 2018b).

Collectively, the small-scale nucleosynthetic isotope variations among bulk meteorites reflect that (i) the protoplanetary disk contained presolar grains with strongly variable isotopic compositions, and (ii) processes occurring in the protoplanetary disk reasonably but not perfectly, mixed these grains into the disk. Moreover, the nucleosynthetic isotope variations are not only useful for identifying the stellar building blocks of the Solar System, but may also provide valuable information about how and to what extent material was transported and mixed in the protoplanetary disk.

14.5 LONG-LIVED AND SHORT-LIVED ISOTOPE CHRONOMETERS

Radiometric isotope dating is a method that determines the chronology of events. An age can be determined by comparing the initial abundance of a radioactive isotope to the abundance of its decay product in material present during the event, where the rate of decay occurs at a known and constant rate (International Union of Pure and Applied Chemistry, 2006). Using this technique, formation age limits are placed on components found in unmelted meteorites (e.g., CAIs and chondrules), as well as on the timescales of differentiation on the parent bodies of melted meteorites. Information on the timescales of parent-body accretion is obtained indirectly, either by dating the formation of a specific component (e.g., chondrules) that is closely linked in time to the accretion of their parent body or, alternatively, by dating a specific chemical differentiation process (e.g., core formation), which can be linked to the time of parent-body accretion through thermal modeling (for reviews see Kleine & Wadhwa, 2017; Kleine & Walker, 2017).

There are two types of chronometers (long-lived and short-lived) that are used to date Solar System and parent body processes. These chronometers are distinguished based on the half-life of the parent isotope. As their parent isotopes have been decaying until the present-day and beyond, long-lived decay systems can provide *absolute* ages. An important example of a long-lived chronometer is the U-Pb system, which provides precise absolute ages of meteorites and their components, provided that they are corrected for variable $^{235}U/^{238}U$ in early Solar System materials (Brennecka et al., 2010). For instance, the Pb–Pb age of CAIs defines the start of the Solar System.

The half-lives of short-lived systems used in cosmochemistry range from ca. 0.1 Ma ($^{41}Ca \rightarrow {}^{41}K$) to ca. 103 Ma ($^{146}Sm \rightarrow {}^{142}Nd$). Short-lived chronometers produce *relative* ages and are usually expressed relative to an age anchor for which precise absolute ages are available. Commonly, this absolute age is taken to be the age of CAIs, as the formation of these materials is taken to reflect the start of the Solar System (Amelin et al., 2002, 2010; Connelly et al., 2012). Short-lived systems are capable of recording events that occurred during the first few 100 Ma of Solar System

https://doi.org/10.1017/9781108856324.018 Published online by Cambridge University Press

history because ingrowth of the daughter nuclide cannot occur after the extinction of the parent nuclide. Long-lived systems may also record these early events; however, these records may be overprinted by younger events, thereby diminishing the utility of long-lived systems for recording events during the first few 100 Ma.

Examples of short-lived chronometers relevant to reconstructing the chronology of events in the early Solar System include the ^{26}Al–^{26}Mg and ^{182}Hf–^{182}W decay systems. Because of the very short half-life of ^{26}Al (t_0 ~0.73 Ma), the Al–Mg system provides very precise relative ages for meteorites and their components. The ^{182}Hf–^{182}W (t_0 ~8.9 Ma; Vockenhuber et al., 2004) system can also be used to obtain relative ages for meteorites and their components, but it is most well-known for its ability to date metal–silicate segregation (e.g., core formation). This application is based on the different geochemical nature of the refractory parent (Hf) and daughter (W) species, where W is moderately siderophile and Hf strongly lithophile. Thus, during core–mantle differentiation a high Hf/W ratio develops in the silicate mantle, whereas a Hf/W of essentially zero develops in the Fe–Ni core. If this segregation of Hf and W occurs during the effective lifetime of ^{182}Hf (~50 Ma, six half-lives), the ^{182}Hf–^{182}W system can provide model ages for the timing of core formation in planetary bodies (for a recent review see Kleine & Walker, 2017).

The application of short-lived chronometers requires robust initial abundances of each parent isotope and their homogeneous distribution in the early Solar System. While most radionuclides (e.g.,^{182}Hf) were homogeneously distributed in the early Solar System, at least at the level relevant for chronological studies, this is debated for ^{26}Al (e.g., Krot et al., 2012; Schiller et al., 2015; Van Kooten et al., 2016). The agreement of Al–Mg and Hf–W ages of meteorites, however, is inconsistent with the presence of significant ^{26}Al heterogeneity at the bulk meteorite scale (Kruijer et al., 2014; Budde et al., 2018).

14.6 THE CARBONACEOUS (CC)–NONCARBONACEOUS (NC) DICHOTOMY

The chemistry and chronology of planet formation can be constrained by documenting the composition and age of a planet's meteoritic building blocks. If these characteristics can be linked to accretion locations in the protoplanetary disk, a time-dependent compositional and spatial "map" of the early Solar System could be constructed. Such information would provide constraints on the composition of the disk, its influence on the composition of the planets, the extent of inner and outer disk mass transfer during planet building, and potentially the origin of volatiles on the terrestrial planets.

The most promising means of obtaining such information is through combined elemental and isotopic analysis of meteorites. A major hurdle, however, is being able to robustly link these (volatile) compositions to physical accretion locations of their parent bodies in the evolving dynamic, three-dimensional protoplanetary disk (Bermingham et al., 2020). As outlined in Chapter 15, although there is a general compositional trend observed in the asteroid belt (dry bodies in the inner belt, more wet bodies in the outer belt), it is unlikely that the asteroids originally accreted in their current location in the belt. On the contrary, the asteroid belt was likely composed of planetesimals that accreted in vastly different regions of the disk but were subsequently implanted in the asteroid belt during gas giant migration and subsequent scattering of planetary bodies (e.g., Walsh et al., 2011; Raymond & Izidoro, 2017; see Chapter 15). As such, the cosmochemical map that the asteroid belt and meteorites seemingly provides may not be as informative as initially envisioned. Recent interpretation of the NC–CC classifications of meteorites and their accretion age, however, has seen the inference of accretion locations of parent bodies, which has led to an integration of meteoritic constraints into large-scale models of disk evolution and planet formation (for recent reviews see Desch et al., 2018; Scott et al., 2018; Kleine et al., 2020; Kruijer et al., 2020).

14.6.1 The NC–CC Dichotomy

To understand the compositional or genetic relationships between meteorites, earlier studies primarily used O isotopes (e.g., Clayton, 1993), where O isotopes variations are likely not nucleosynthetic in origin and instead reflect photochemical processes in the protoplanetary disk or the molecular cloud (for a review of O isotopes, see Ireland et al., 2020). Over the past few decades, several studies demonstrated that carbonaceous chondrites are isotopically distinct in O isotopes and in heavier isotopes (e.g., ^{50}Ti, ^{54}Cr, ^{58}Ni) from ordinary and enstatite chondrites, several achondrite groups (including the HED meteorites), and the Earth, Moon, and Mars (Niemeyer, 1988; Rotaru et al., 1992; Clayton, 1993; Trinquier et al., 2007; Leya et al., 2008; Regelous et al., 2008). The fundamental nature of this finding with regards to the evolution of the protoplanetary disk was first recognized by Warren (2011). The author coined the terms NC and CC and suggested that, given the Earth, Moon, and Mars have compositions which fall within the NC field, NC meteorites probably come from an inner Solar System reservoir. In contrast, because some of the more volatile-rich CC meteorites were considered to come from the outer Solar System, CC meteorites probably come from an outer Solar System reservoir (for a recent review of some of the complexities involved, see Bermingham et al., 2020). Warren (2011) postulated that the NC and CC regions were separated by proto-Jupiter. The genetic dichotomy has since been interpreted as a pervasive division of meteorites into NC and CC meteorites.

The NC–CC dichotomy is most clearly observed when different nucleosynthetic tracers (e.g., ^{50}Ti versus ^{54}Cr) are plotted against each other (Figure 14.1) and two distinct compositional fields become apparent. Recently, it has become apparent that the NC–CC dichotomy extends to several other isotope systems (e.g., siderophile elements Mo, Ru, W) and meteorite groups (achondrites, grouped and ungrouped iron meteorites, pallasites) (e.g., Budde et al., 2016; Kruijer et al., 2017; Poole et al., 2017; Worsham et al., 2017, 2019; Bermingham et al., 2018b; Hilton et al., 2019; Tornabene et al., 2020). Despite isotopic variations within the individual NC and CC reservoirs, there is a gap in between the two groups which complicates the possibility of grouping representing a mixing continuum in compositions. Rather it implies minimal to absent mixing between the NC and CC reservoirs during the formation times of the meteorite parent bodies.

Several publications have investigated the NC–CC isotope dichotomy using nucleosynthetic isotope variations defined by

https://doi.org/10.1017/9781108856324.018 Published online by Cambridge University Press

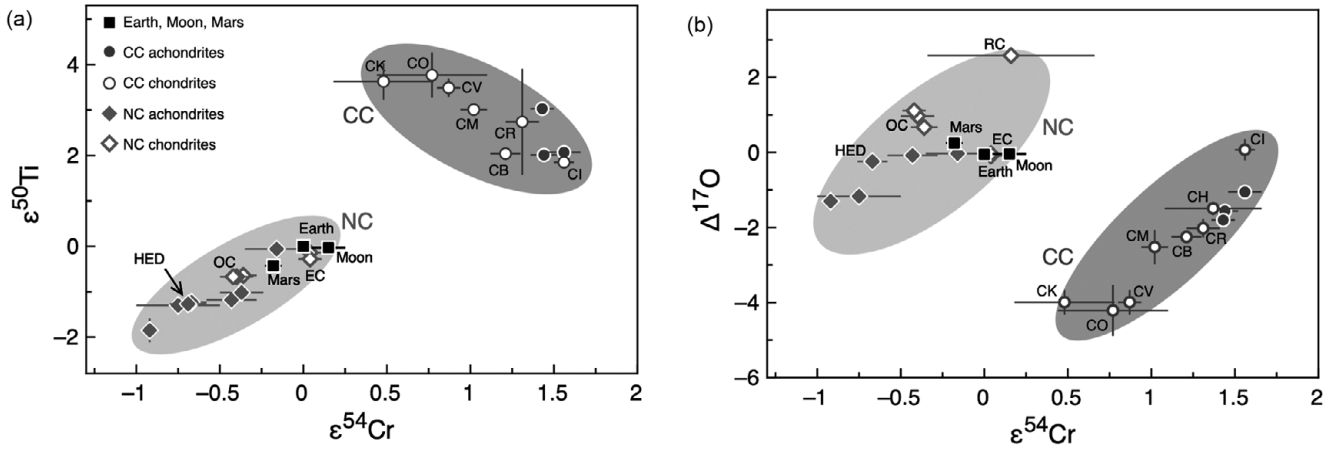

Figure 14.1 NC–CC meteorite dichotomy inferred from isotopic signatures of bulk meteorites. (a) ε^{50}Ti versus ε^{54}Cr, (b) Δ^{17}O versus ε^{54}Cr. Note that 1 ε-unit represents the 0.01% deviation (and 1 δ-unit the 0.1% deviation) in the isotopic ratio of a sample relative to terrestrial rock standards. Mass-independent O isotope variations are expressed in $\Delta^{17}O$ ($\Delta^{17}O \equiv \delta^{17}O - 0.52\ \delta^{18}O$, where 0.52 is the slope of mass-dependent mass fractionation). Errors bars denote external uncertainties (2σ) reported in respective studies. The isotopic data shown are based on that initially summarized in Warren (2011) with several updates (see Kruijer et al., 2020, and references therein).

lithophile and siderophile elements (e.g., Desch et al., 2018; Scott et al., 2018; Alexander, 2019a, 2019b). The rest of this section primarily focuses on recent advances made through the isotopic analysis of siderophile elements Ni, Mo, Ru, and W, which provide information on the origin and dynamical implications of the NC–CC dichotomy.

Nucleosynthetic isotope variations observed for Mo are particularly illustrative because, unlike for elements such as Ti and Cr, the isotopic composition of Mo has been precisely analyzed in almost all classes of meteorites. Moreover, Mo isotopes permit isotopic anomalies of distinct nucleosynthetic origins to be distinguished. Specifically, the heterogeneous distribution of carriers enriched in nuclides produced in the *s*-process of stellar nucleosynthesis (often associated with asymptotic giant branch, AGB, stars) and the rapid neutron capture process *r*-process (associated with neutron-rich stellar environments, such as supernovae or neutron star merger events) yields different patterns of Mo isotope anomalies within individual samples (Dauphas et al., 2002; Burkhardt et al., 2011).

Although nucleosynthetic Mo isotope variations have received interest for almost two decades, several recent high-precision Mo isotope studies have greatly expanded the available data for bulk meteorites (e.g., Kruijer et al., 2017; Poole et al., 2017; Worsham et al., 2017, 2019; Bermingham et al., 2018a, 2018b; Budde et al., 2019; Hilton et al., 2019; Tornabene et al., 2020). For Mo, the NC–CC dichotomy is most clearly seen in a plot of ε^{94}Mo versus ε^{95}Mo, where stony, stony iron, and iron NC and CC meteorites define two approximately parallel *s*-process mixing lines which are offset from each other (Figure 14.2) (Budde et al., 2016; Kruijer et al., 2017; Poole et al., 2017; Worsham et al., 2017; Hilton et al., 2019; Yokoyama et al., 2019; Tornabene et al., 2020). Why this difference in NC and CC Mo isotope compositions persists remains debated. This offset has been considered to reflect an approximately homogeneous enrichment in *r*-process (and possibly *p*-process) nuclides in the CC compared to the NC reservoir (Budde et al., 2016; Kruijer et al., 2017; Poole et al., 2017; Worsham et al., 2017). Regardless of the cause of the isotopic difference between the NC and CC groups, the bimodality is found in many bulk meteorite samples and thus appears to record a fundamental property of the protoplanetary disk.

Whereas the *s*-process variability in each reservoir can potentially be controlled by individual presolar carrier phases (or derivatives thereof), the homogeneous enrichment in *r*-process Mo in the CC over the NC reservoir cannot. It has been interpreted to be a characteristic composition of the entire CC reservoir (Budde et al., 2016; Worsham et al., 2017, 2019; Burkhardt et al., 2019; Nanne et al., 2019). A key finding based on the Mo isotope data is that the NC and CC reservoirs do not only contain chondrites, but also iron meteorites and pallasites (Kruijer et al., 2017; Poole et al., 2017; Worsham et al., 2017; Bermingham et al., 2018b; Hilton et al., 2019; Tornabene et al., 2020) and other achondrites (Worsham et al., 2017, 2019; Budde et al., 2019). For both the NC and CC reservoirs, iron meteorites and chondrites plot on single s-process mixing lines (i.e., the NC- and CC-lines), implying that CC irons, achondrites, and carbonaceous chondrites have the same characteristic *r*-process excess over the NC irons and enstatite and ordinary chondrites.

The dichotomy exists for elements covering a wide range of condensation temperatures (non-refractory elements like Cr and Ni, as well as refractory elements such as Ni, Mo, Ru, and W) and both for lithophile (Ti, Cr) and siderophile (Ni, Mo, Ru, W) elements. As the NC–CC dichotomy exists for elements covering a broad range of geochemical and cosmochemical behavior, the dichotomy may indicate a ubiquitous characteristic of the protoplanetary disk. For some element pairs, nucleosynthetic isotope signatures are correlated in one reservoir but not the other (Worsham et al., 2019). For example, W and Mo isotope signatures show correlations for CC, but not for CC meteorites, whereas Mo and Ru isotope signatures are correlated in the NC but not the CC reservoir. These more complex inter-element isotope relationships may reflect distinct redox and thermal conditions at which presolar carrier phases were processed in the individual reservoirs (Burkhardt et al., 2012; Fischer-Gödde et al., 2015). This observation suggests that the CC reservoir may have been characterized by more oxidizing conditions

https://doi.org/10.1017/9781108856324.018 Published online by Cambridge University Press

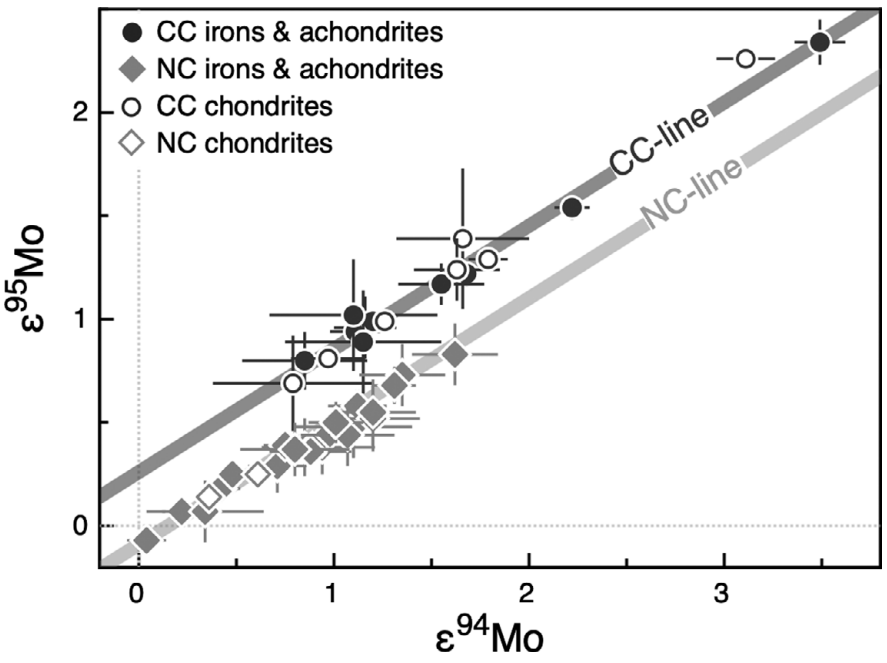

Figure 14.2 ε^{95}Mo versus ε^{94}Mo data for bulk meteorites. NC (grey) and CC (black) meteorites define two approximately parallel *s*-process mixing lines with identical slopes, but distinct intercept values (Budde et al., 2016, 2019; Kruijer et al., 2017). Error bars denote external uncertainties reported in respective studies (2σ).

than the NC reservoir (Worsham et al., 2019). If this differential volatility model is supported by elemental compositions remains an open question exceptions include iron meteorite Wiley and members of the IIC iron meteorite group (Tornabene et al., 2020). These samples have chemical and isotopic compositions that reflect either selective thermal processing of nucleosynthetic carriers, or are genetically distinct from the CC and NC precursor materials (Tornabene et al., 2020).

Collectively, isotopic data reveal that the NC–CC dichotomy exists widely, demonstrating that the NC–CC dichotomy is a fundamental characteristic of the meteorite record. The dichotomy indicates that the NC and CC meteorites stem from different reservoirs that did not mix, or only very minimally mixed during the formation period of meteorite parent bodies. As will be illustrated, the discovery of the NC–CC dichotomy, combined with a precise chronology for the accretion of meteorite parent bodies, has led to new large-scale models of disk evolution and planet formation.

14.7 NC–CC DICHOTOMY: IMPLICATIONS FOR THE STRUCTURE AND DYNAMICAL EVOLUTION OF THE EARLY SOLAR SYSTEM

Given the predominance of the NC–CC grouping in meteorites, the dichotomy may provide a fundamental constraint on the structure and dynamical evolution of the early Solar System. The dichotomy has been interpreted to reflect the formation of meteorite parent bodies in two spatially separated regions in the disk. Understanding the significance of the NC-CC grouping requires knowledge of the accretion times of NC and CC meteorite parent bodies. Such information can be obtained from the chronology of meteorites and their components. This section focuses on those ages that provide the most precise constraints on the accretion timescales of NC and CC meteorite parent bodies, rather than providing a comprehensive summary of the chronology of meteorites.

14.7.1 Chronology of NC and CC Meteorites

14.7.1.1 Differentiated (or Melted) Meteorites

Collectively, meteorite ages demonstrate that planetesimal differentiation occurred within the first few million years after CAI formation, consistent with heating driven mainly by ^{26}Al decay. Direct evidence for early planetesimal differentiation comes from the ^{182}Hf–^{182}W chronometry of magmatic iron meteorites.

Model ages obtained using the ^{182}Hf–^{182}W system indicate that magmatic iron meteorite parent bodies segregated their cores very early in Solar System history, between ca. 0.5 and 3 Ma after Solar System formation (Kruijer et al., 2014, 2017). Although the ^{182}Hf–^{182}W ages of NC and CC iron meteorite groups are not clearly resolved outside their uncertainties (Hellmann et al., 2019; Hilton et al., 2019; Kruijer & Kleine, 2019), the Hf–W chronology of iron meteorites demonstrate that core formation on their parent bodies occurred around ∼0.5–2 Ma (NC irons) and ∼2–3 Ma (CC irons) after CAI formation (Kruijer et al., 2014, 2017, 2020). Combining the ^{182}Hf–^{182}W ages of iron meteorites with thermal modeling for small bodies heated by ^{26}Al decay yields accretion ages for iron meteorite parent bodies of ∼0.5 Ma (NC irons) and ∼1 Ma (CC irons) after CAI formation, with some overlap in accretion age between NC and CC parent bodies (Hilton et al., 2019). Iron meteorite parent bodies, therefore, accreted within <1 Ma after Solar System formation and are among the first planetesimals formed in the Solar System preserved in the meteorite collection.

https://doi.org/10.1017/9781108856324.018 Published online by Cambridge University Press

In principle, accretion and core formation timescales can also be inferred for the parent bodies of differentiated achondrites (e.g., eucrites, angrites, ureilites). These accretion ages, however, are less well constrained than those of iron meteorites, because additional parent–daughter (e.g., ^{182}Hf–^{182}W or ^{26}Al–^{26}Mg) chemical fractionation events in the silicate mantles after core formation can complicate the chronology recorded by the radiometric systems. The isotopic compositions of these samples may, therefore, reflect more than one differentiation event, thereby adding substantial uncertainty to the model ages for core formation. Nevertheless, the available data are most consistent with early core formation on the angrite and eucrite parent bodies, well within the first ~1–2 Ma of the Solar System (Bizzarro et al., 2005; Kleine et al., 2012; Touboul et al., 2015), and thus approximately as early as the iron meteorite parent bodies. This is consistent with thermal models for the early evolution of Vesta that also predict a very early formation (Formisano et al., 2013; Neumann et al., 2014). Collectively the meteorite data indicate that Vesta and the angrite and ureilite parent bodies likely accreted and segregated its core very early in the history of the Solar System. Note that the timing of subsequent minor additions of CC materials to Vesta remains unconstrained by the meteorite data.

14.7.1.2 Undifferentiated (or Unmelted) Meteorites: Chondrules

The accretion of undifferentiated parent bodies of chondrites cannot be dated directly but must instead be inferred by dating individual meteorite components that formed just prior to or during accretion of their host chondrite (Alexander et al., 2008). Of these components, chondrules are the most abundant as well as most extensively dated component (see e.g., Krot et al., 2018, and references therein). Radiometric ages of chondrules are obtained either by pooling multiple chondrules (Pb–Pb, Hf–W) or by dating individual chondrules (Pb–Pb, Al–Mg,). Perhaps the strongest constraint comes from ^{26}Al–^{26}Mg chronometry of individual chondrules from the least altered chondrites, which yields clear age peaks at ~2–3 Ma (for chondrules from ordinary, CV, and CO chondrites) and at ~3.7 Ma (CR chondrites), after CAI formation (Villeneuve et al., 2009; Kita & Ushikubo, 2012; Nagashima et al., 2017; Schrader et al., 2017; Pape et al., 2019). These ages are in excellent agreement with ^{182}Hf–^{182}W (Budde et al., 2016, 2018) and Pb–Pb ages of pooled chondrule separates from CV and CR chondrites (Amelin et al., 2002; Amelin & Krot, 2007; Connelly et al., 2008; Connelly & Bizzarro, 2009). Thus, the vast majority of chondrules formed between ~2 and ~4 Ma after CAI formation. Moreover, chondrules from a given chondrite group formed in a narrow time span of <1 Ma, suggesting they rapidly accreted into their parent bodies. This inferred narrow time interval of chondrule formation is also supported by independent evidence from the chronology of secondary alteration products (for example, carbonates and secondary fayalites; e.g., Doyle et al., 2015; Jogo et al., 2017) as well as with studies combining meteorite chronology with thermal modeling of bodies by ^{26}Al decay (Henke et al., 2012; Blackburn et al., 2017; Hellmann et al., 2019). This suggests that the ^{26}Al–^{26}Mg chondrule ages are chronologically meaningful, which implies that the chondrule ages closely approximate the time of chondrite parent body accretion.

The Pb–Pb ages for individual chondrules from ordinary, CV, and CR chondrites, however, are more variable and some even appear to be as old as CAIs (Connelly et al., 2012; Bollard et al., 2017). These authors suggested that the discrepancy between the Al–Mg and Pb–Pb ages reflects local variations of ^{26}Al/^{27}Al in the disk, and specifically, a reduced initial ^{26}Al/^{27}Al in the inner Solar System (Bollard et al., 2019). This interpretation, however, is difficult to reconcile with the good agreement between Hf–W and Al–Mg ages for several meteorites and meteorite components. This includes samples with formation ages varying by almost 5 Ma and materials stemming from both the inner (NC) and outer (CC) disk (Budde et al., 2018; Kleine et al., 2020; Kruijer et al., 2020). Thus, the discrepancy between Al–Mg and Pb–Pb ages for single chondrules cannot be caused by spatial heterogeneities of ^{26}Al/^{27}Al. Another possibility to explain this discrepancy is that the Pb–Pb ages were shifted toward older ages due to the loss of intermediate decay products within the U–Pb decay chains (Pape et al., 2019). Nevertheless, regardless of the variable Pb–Pb ages reported for some individual chondrules and the exact origin for these variations, there is strong evidence that the vast majority of chondrules formed between ~2 and ~4 Ma after CAI formation. Thus, collectively, the available Al–Mg, U–Pb, and Hf–W chronology of chondrules indicates that chondrite parent body accretion in both the NC and CC reservoirs occurred later than that of iron meteorites, around ~2 Ma in the NC reservoir (ordinary chondrites) and continuing until at least ~4 Ma after CAI formation in the CC reservoir (CR chondrites).

14.7.2 Time of Formation and Lifetime of the NC–CC Dichotomy

Combined, the chronology of meteorite parent body accretion indicates that meteorite parent body accretion in both NC and CC reservoirs (i) commenced within <1 Ma after CAI formation and (ii) lasted several Ma, up to at least 2 Ma in the NC reservoir and up to ~4 Ma in the CC reservoir. A key observation is that the NC- or CC-characteristic isotopic signatures of their respective nebular reservoirs were not significantly modified during this period. This is evident in the observation that early formed iron meteorites and later-formed chondrites plot on two individual *s*-process mixing lines in Mo isotope space (Figure 14.2). Even though the Mo isotopic data reveal small deviations from each line (Yokoyama et al., 2019), these differences are small compared to the overall offset between the NC- and CC-lines (Spitzer et al., 2020). Combined, the nucleosynthetic signatures and ages of NC and CC meteorites thus suggest that there was minimal influx of CC matter into the NC reservoir between ~0.5 and ~2 Ma after CAI formation, and negligible influx of NC matter into the CC reservoir between ~1 and ~4 Ma after CAIs. Collectively, the isotopic data indicate the presence of two co-existing and spatially separated NC and CC reservoirs for several Ma (Kruijer et al., 2017).

14.7.3 Possible Mechanisms for the NC–CC Isotopic Divide and the Jupiter Barrier

The spatial separation of NC and CC reservoirs inferred from the isotopic data requires an efficient mechanism preventing the radial exchange of NC and CC materials (Figure 14.3). One way to retain

https://doi.org/10.1017/9781108856324.018 Published online by Cambridge University Press

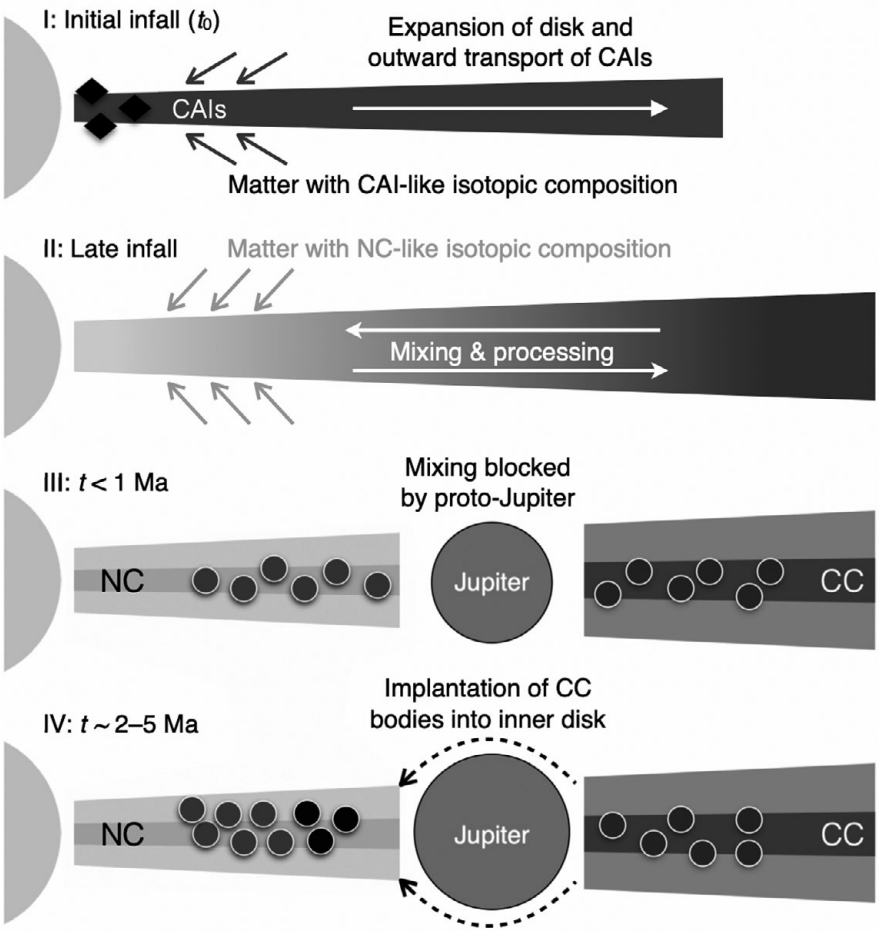

Figure 14.3 Postulated evolution of the solar accretion disk. Initially (Stages I and II, $t \sim 0$ Ma after Solar System formation) the disk grew and facilitated relatively rapid transport and mixing of nebular dust. The growth of proto-Jupiter (Stage III, $t < 1$ Ma), however, may have acted as a barrier against material transport, preserving any pre-existing isotope difference between NC and CC materials. This would have been followed (Stage IV, $t \sim 2$–5 Ma) by the opening of a gap within the disk and/or Jupiter's migration. In either case, Jupiter's growth likely facilitated the inward scattering of planetesimals and their implantation into the main asteroid belt region.

Figure modified after Nanne et al. (2019) and Kruijer et al. (2020)

the NC–CC isotope dichotomy over several Ma is the rapid accretion of dust into planetesimals with more stable orbits, which might have prevented exchange of dust between the NC and CC reservoirs. This mechanism, however, does not explain the observation that meteorite parent bodies with the same characteristic NC–CC isotopic difference continued to accrete for several Ma. Rapid radial transport and mixing of dust in the disk would have homogenized the NC–CC isotopic difference in a much shorter period (Weidenschilling, 1977; Birnstiel et al., 2013). Alternatively, if it is assumed that the NC group formed in the inner Solar System and the CC formed in the outer Solar System, a spatial separation of NC and CC reservoir may have developed due to the early formation of proto-Jupiter. The formation of Jupiter could have prevented material transport between the inner and outer disk in two ways, either by the growth of Jupiter itself (Warren, 2011; Morbidelli et al., 2016; Kruijer et al., 2017) or alternatively through a pressure maximum or dust trap at the orbital distance where Jupiter subsequently formed (Brasser & Mojzsis, 2020). The early presence of proto-Jupiter could have prevented the inward and outward transport of dust grains after it had reached ca. 10–20 Earth masses (Lambrechts & Johansen, 2012; Alibert et al., 2018), and thus eventually divided the early disk into two separate NC and CC regions with limited mixing between them (Kruijer et al., 2017). If correct, the ancient accretion ages obtained for NC and CC iron meteorites indicate that the Jupiter barrier was present very early, within <1 Ma after CAI formation (Figure 14.3, Stage 3). This would imply that Jupiter is the oldest planet of the Solar System, and the solid core of Jupiter must have formed well within ~1 Ma after CAI formation.

In detail, the efficacy of the Jupiter barrier depends on the grain size of the dust drifting inwards and the size and growth history of Jupiter. The Jupiter barrier may have resulted in a filtering effect, that allowed small (ca. 100 μm sized) dust grains to pass through, but efficiently hampered the drift of larger (ca. mm-sized) grains (Weber et al., 2018). This filtering process may have imparted small isotopic changes within the NC reservoir, as seen in ε^{50}Ti versus ε^{54}Cr space (Figure 14.1) as well as in nucleosynthetic Mo (Spitzer et al., 2020) and Ca isotope signatures (Schiller et al., 2018). Hence, one possibility is that the isotopic composition of the inner Solar System might have changed continuously through the addition of CC dust. Alternatively, the small isotopic variations among NC meteorites record a rapidly changing composition of the disk during infall from the Sun's parental molecular cloud, where

https://doi.org/10.1017/9781108856324.018 Published online by Cambridge University Press

each planetesimal locks the instant composition of the disk when it forms (Nanne et al., 2019; Spitzer et al., 2020). An important implication of the infall model is that later accreted planetesimals in the inner disk primarily formed from secondary dust produced by collisions among pre-existing NC planetesimals.

The early growth of Jupiter is consistent with a previously proposed mechanism for the implantation of carbonaceous chondrites parent bodies from the outer disk into the inner disk (e.g., Walsh et al., 2011). This is because the subsequent growth of Jupiter (to ca. 50 Earth masses) would eventually have led to the formation of a gap within the disk (Crida et al., 2006). This likely ultimately led to inward migration of Jupiter and gravitational scattering of outer Solar System parent bodies from beyond its orbit into the inner Solar System (Walsh et al., 2011; Raymond & Izidoro, 2017a) (Figure 14.3, Stage 4). Although the exact timing remains somewhat uncertain, the available isotopic data of NC and CC meteorites suggest that migration and inward scattering of CC bodies occurred between ~2 and ~5 Ma after CAI formation (Kruijer et al., 2017, 2020). Consistent with this, a recent study identified one meteorite with a mixed NC–CC isotopic composition that was established relatively late, implying that it may have formed by collisional mixing of NC and CC planetesimals (Spitzer et al., in press). The implantation of CC bodies into the inner Solar System probably led to mixing of CC and NC materials from this time onward. Jupiter subsequently grew to its final size (~318 Earth masses) because of gas accretion onto its core (Pollack et al., 1996), which must have happened prior to dissipation of the nebular gas, probably ~4–5 Ma. The inferred timescale for Jupiter's growth based on cosmochemical data is consistent with predictions from the core accretion model for giant planet formation (Pollack et al., 1996; Alibert et al., 2018).

14.7.4 Origin of the NC–CC Dichotomy

Although the cause of the isotopic difference between the NC and CC reservoirs is still debated, three key characteristics of the NC–CC meteorite dichotomy provide important clues about its origin. First, the dichotomy exists for elements with a wide range of condensation temperatures, including refractory (e.g., Ti, Mo, W) and non-refractory and/or volatile elements (e.g., Cr, Ni). Second, the CC reservoir is relatively enriched in nuclides produced in neutron-rich stellar environments, as demonstrated by excesses in ^{50}Ti, ^{54}Cr, ^{58}Ni, and *r*-process Mo. Third, similar but more pronounced enrichments in neutron rich isotopes are found in CAIs (Papanastassiou, 1986; Burkhardt et al., 2011; Brennecka et al., 2013; Davis et al., 2018), the oldest objects of the Solar System. From these observations, it seems unlikely the NC–CC dichotomy reflects preferential destruction and volatilization of isotopically anomalous material through locally elevated temperatures within the disk (e.g., Trinquier et al., 2009; Burkhardt et al., 2011), because this would have resulted in disparate effects on carriers of elements with different volatilities (Nanne et al., 2019). In addition, such thermal processing would not selectively affect carriers from specific neutron-rich stellar environments. Instead, it has been suggested that the NC–CC dichotomy reflects an isotopic heterogeneity in the disk that was imparted during heterogeneous infall from the molecular cloud (Burkhardt et al., 2019; Jacquet et al., 2019; Nanne et al., 2019; Figure 14.3, Stages I and II). In these models, the earliest solar accretion disk, which formed by viscous spreading of early infalling matter (Yang & Ciesla, 2012; Desch et al., 2018; Jacquet et al., 2019), would have had a CAI-like isotopic composition, and be enriched in nuclides produced in neutron rich stellar environments. Note that this earliest disk would not only have contained refractory materials (e.g., CAIs) but also other, non-refractory, dust particles. In contrast, later infalling matter primarily was added to the inner disk and the inner disk thus retained its obtained NC-like isotopic composition. Mixing of these two end member sources within the disk subsequently generated the CC reservoir with an isotopic composition that is intermediate between early (CAI-like) and late-infalling (NC-like) material (Burkhardt et al., 2019; Nanne et al., 2019; Spitzer et al., 2020). After infall had ended, the proto-Sun continued to accrete material from the outer disk (Yang & Ciesla, 2012). Thus, to preserve the isotopic difference between the inner (NC) and outer (CC) reservoirs a barrier is required that efficiently inhibits radial transport of CC material into the inner disk. As mentioned in Section 14.7.3, the most plausible mechanism for such an efficient separation of NC and CC disk reservoirs is the growth of Jupiter or, alternatively, the presence of a pressure bump where Jupiter subsequently formed.

14.8 GENETIC HERITAGE OF VESTA AND CERES

Clues about the genetic heritage of Vesta come from the nucleosynthetic signatures of HED meteorites. The ε^{50}Ti and ε^{54}Cr isotope signatures reveal that HED meteorites fall within the field of NC meteorites (Figures 14.1 and 14.2), making the HED meteorites and Vesta a very early accreted and differentiated NC body. Previous studies have identified exogenic carbonaceous chondrite-like signatures in the regolith of Vesta (e.g., De Sanctis et al., 2012; Jaumann et al., 2012; McCord et al., 2012; Prettyman et al., 2012; Reddy et al., 2012; Lunning et al., 2016; Chapter 6). These CC materials are not endogenous to Vesta and may have come from an impactor that formed Vesta's Veneneia (diameter 400 ± 20 km) impact basin which is superimposed on Rheasilvia (diameter 500 ± 20 km) (Jaumann et al., 2012; Reddy et al., 2012; Schenk et al., 2012; Lunning et al., 2016).

Searching for endogenous water on Vesta and the angrite parent body, Sarafian et al., (2014, 2017a, 2017b) concluded that the similarity between the H isotope compositions of HED (and angrite) meteorites (Barrett et al., 2016) and bulk carbonaceous chondrites indicated that water was acquired by the accretion of carbonaceous chondrite material onto these parent bodies while they were still partially molten (see review by Alexander et al., 2018). Sarafian et al. (2017a, 2017b) concluded that Vesta and the angrite parent body acquired the majority of their water content earlier than 5 Ma. Sarafian et al. (2019) recently reported a bulk H_2O (10–70 ppm) and fluorine (0.3–2 ppm) composition of Vesta determined from unequilibrated eucrites, where the D/H of these samples also match CC material. These authors built on work by Humayun and Clayton (1995), Righter (2007), and Day and Moynier (2014) to investigate the idea that inner Solar System material accumulated water during accretion and retained water and possibly other volatile elements proportional to their size. If so, this would indicate that there was some indigenous water in the inner (NC) Solar System that imparted low volatile concentrations on some asteroids including Vesta. Authors, however, conclude that the isotopic composition

https://doi.org/10.1017/9781108856324.018 Published online by Cambridge University Press

of unequilibrated eucrites is consistent with a chondritic source of volatile elements to early forming Vesta.

As Ceres has not been linked to any known meteorite group, it is currently not possible to confirm if Ceres belongs to the NC or CC meteorite reservoir. Nevertheless, given that Ceres has a C-rich and ammonia-rich surface, is modeled to have relatively large amounts of macromolecular organic matter, and is more water-rich than known "wet" meteorites (e.g., CI chondrites) (see e.g., Prettyman et al., 2012, 2017; De Sanctis et al., 2016; Carrozzo et al., 2018; as well as Chapters 7, 8–9), it is likely that Ceres is a CC asteroid which initially formed in the outer Solar System and was then implanted into the inner Solar System during giant planet migration (see Chapter 15). Alternatively, Ceres may be an asteroid which originally accreted in the NC reservoir and either accreted significantly more water and volatiles that Vesta, or Ceres' chemical composition was subsequently modified through late accretion of more organic and volatile rich material derived from the CC reservoir. These later accreted materials may then either have been added through inward drift of small CC dust during the lifetime of the NC–CC bodies or, alternatively, may reflect the later implantation of CC-like bodies into the inner Solar System that mixed with NC bodies at a later stage.

14.9 CONCLUDING REMARKS

Nucleosynthetic and radiogenic isotope signatures of melted and unmelted meteorites are currently used to infer a compositional and temporal map of protoplanetary disk's evolution into the planets. Although questions remain about the confidence with which these meteorite compositions can be linked to accretion locations in the disk, the combination of nucleosynthetic and radiogenic isotope data suggest that the inner and outer protoplanetary disk underwent early segregation to form the NC–CC regions, possibly by the formation of proto-Jupiter. This segregation event likely limited the movement of material from the inner and outer disk, thereby strongly influencing the diversity of material available for planetary formation in the different regions. Although the communication between the NC and CC reservoirs appears to be limited, the volatile content of some asteroids suggests that some outer Solar System material may have breached this early divide. Although the details remain to be investigated, such additions of CC bodies to the inner Solar System could either have been accommodated by inward drift of small CC dust during the lifetime of NC–CC dichotomy or, alternatively, by the later implantation of CC bodies into inner Solar System. How this movement of outer Solar System material may have happened without significant modification of the NC–CC isotopic indicia and if this played a role in the origin of Earth's volatile content remain open questions that can be addressed by future analysis of main asteroid belt materials.

REFERENCES

Alexander, C. M. O. (2019a) Quantitative models for the elemental and isotopic fractionations in chondrites: The carbonaceous chondrites. *Geochimica et Cosmochimica Acta*, 254, 277–309.

Alexander, C. M. O. (2019b) Quantitative models for the elemental and isotopic fractionations in the chondrites: The non-carbonaceous chondrites. *Geochimica et Cosmochimica Acta*, 254, 246–276.

Alexander, C. M. O., Grossman, J. N., Ebel, D. S., & Ciesla, F. J. (2008) The formation conditions of chondrules and chondrites. *Science*, 320, 1617–1619.

Alexander, C. M. O., McKeegan, K. D., & Altwegg, K. (2018) Water reservoirs in small planetary bodies: Meteorites, asteroids, and comets. *Space Science Reviews*, 214, 36.

Alibert, Y., Venturini, J., Helled, R., et al. (2018) The formation of Jupiter by hybrid pebble–planetesimal accretion. *Nature Astronomy*, 2, 873–877.

Amelin, Y., Kaltenbach, A., Iizuka, T., et al. (2010) U–Pb chronology of the Solar System's oldest solids with variable $^{238}U/^{235}U$. *Earth and Planetary Science Letters*, 300, 343–350.

Amelin, Y., & Krot, A. (2007) Pb isotopic age of the Allende chondrules. *Meteoritics & Planetary Science*, 42, 1321–1335.

Amelin, Y., Krot, A. N., Hutcheon, I. D., & Ulyanov, A. A. (2002) Lead isotopic ages of chondrules and calcium-aluminum-rich inclusions. *Science*, 297, 1678.

Barrett, T. J., Barnes, J. J., Tartèse, R., et al. (2016) The abundance and isotopic composition of water in eucrites. *Meteoritics & Planetary Science*, 51, 1110–1124.

Benedix, G. K., McCoy, T. J., Keil, K., & Love, S. G. (2000) A petrologic study of the IAB iron meteorites: Constraints on the formation of the IAB-winonaite parent body. *Meteoritics & Planetary Science*, 35, 1127–1141.

Bermingham, K. R., Füri, E., Lodders, K., & Marty, B. (2020) The NC–CC isotope dichotomy: Implications for the chemical and isotopic evolution of the early Solar System. *Space Science Reviews*, 216, 133.

Bermingham, K. R., Gussone, N., Mezger, K., & Krause, J. (2018a) Origins of mass-dependent and mass-independent Ca isotope variations in meteoritic components and meteorites. *Geochimica et Cosmochimica Acta*, 226, 206–223.

Bermingham, K. R., Mezger, K., Scherer, E. E., et al. (2016) Barium isotope abundances in meteorites and their implications for early Solar System evolution. *Geochimica et Cosmochimica Acta*, 175, 282–298.

Bermingham, K. R., Worsham, E. A., & Walker, R. J. (2018b) New insights into Mo and Ru isotope variation in the nebula and terrestrial planet accretionary genetics. *Earth and Planetary Science Letters*, 487, 221–229.

Binzel, R. P., & Xu, S. (1993) Chips off of asteroid 4 Vesta: Evidence for the parent body of basaltic achondrite meteorites. *Science*, 260, 186.

Birnstiel, T., Dullemond, C. P., & Pinilla, P. (2013) Lopsided dust rings in transition disks. *Astronomy & Astrophysics*, 550, L8.

Bizzarro, M., Baker, J. A., Haack, H., & Lundgaard, K. L. (2005) Rapid timescales for accretion and melting of differentiated planetesimals inferred from ^{26}Al–^{26}Mg chronometry. *Astrophysics Journal*, 632, L41–L44.

Blackburn, T., Alexander, C. M. O., Carlson, R., & Elkins-Tanton, L. T. (2017) The accretion and impact history of the ordinary chondrite parent bodies. *Geochimica et Cosmochimica Acta*, 200, 201–217.

Blum, J., & Wurm, G. (2000) Experiments on sticking, restructuring, and fragmentation of preplanetary dust aggregates. *Icarus*, 143, 138–146.

Bollard, J., Connelly, J. N., Whitehouse, M. J., et al. (2017) Early formation of planetary building blocks inferred from Pb isotopic ages of chondrules. *Science Advances*, 3, e1700407.

Bollard, J., Kawasaki, N., Sakamoto, N., et al. (2019) Combined U-corrected Pb–Pb dating and ^{26}Al–^{26}Mg systematics of individual chondrules – Evidence for a reduced initial abundance of ^{26}Al amongst inner Solar System chondrules. *Geochimica et Cosmochimica Acta*, 260, 62–83.

Brasser, R., & Mojzsis, S. J. (2020) The partitioning of the inner and outer Solar System by a structured protoplanetary disk. *Nature Astronomy*, 4, 492–499.

Brennecka, G. A., Borg, L. E., & Wadhwa, M. (2013) Evidence for supernova injection into the solar nebula and the decoupling of *r*-process nucleosynthesis. *Proceedings of the National Academy of Sciences (USA)*, 110, 17241.

Brennecka, G. A., Weyer, S., Wadhwa, M., et al. (2010) 238U/235U Variations in meteorites: Extant 247Cm and implications for Pb–Pb dating. *Science*, 327, 449–451.

Buchwald, V. F. (1975) *Handbook of Iron Meteorites: Their History, Distribution, Composition, and Structure, in 3 volumes*. Berkeley: University of California Press.

Budde, G., Burkhardt, C., Brennecka, G. A., et al. (2016) Molybdenum isotopic evidence for the origin of chondrules and a distinct genetic heritage of carbonaceous and non-carbonaceous meteorites. *Earth and Planetary Science Letters*, 454, 293–303.

Budde, G., Burkhardt, C., & Kleine, T. (2019) Molybdenum isotopic evidence for the late accretion of outer Solar System material to Earth. *Nature Astronomy*, 3, 736–741.

Budde, G., Kruijer, T. S., & Kleine, T. (2018) Hf-W chronology of CR chondrites: Implications for the timescales of chondrule formation and the distribution of ^{26}Al in the solar nebula. *Geochimica et Cosmochimica Acta*, 222, 284–304.

Burbine, T. H. (1998) Could G-class asteroids be the parent bodies of the CM chondrites? *Meteoritics & Planetary Science*, 33, 253–258.

Burkhardt, C., Dauphas, N., Hans, U., Bourdon, B., & Kleine, T. (2019) Elemental and isotopic variability in Solar System materials by mixing and processing of primordial disk reservoirs. *Geochimica et Cosmochimica Acta*, 261, 145–170.

Burkhardt, C., Kleine, T., Dauphas, N., & Wieler, R. (2012) Origin of isotopic heterogeneity in the solar nebula by thermal processing and mixing of nebular dust. *Earth and Planetary Science Letters*, 357–358, 298–307.

Burkhardt, C., Kleine, T., Oberli, F., et al. (2011) Molybdenum isotope anomalies in meteorites: Constraints on solar nebula evolution and origin of the Earth. *Earth and Planetary Science Letters*, 312, 390–400.

Cameron, A. G. W., & Truran, J. W. (1977) The supernova trigger for formation of the Solar System. *Icarus*, 30, 447–461.

Carrozzo, F. G., De Sanctis, M. C., Raponi, A., et al. (2018) Nature, formation, and distribution of carbonates on Ceres. *Science Advances*, 4, e1701645.

Clayton, D. D. (1982) Cosmic chemical memory: a new astronomy. *Quarterly Journal of the Royal Astronomical Society*, 23, 174–212.

Clayton, R. N. (1993) Oxygen isotopes in meteorites. *Annual Review of Earth and Planetary Sciences*, 21, 115–149.

Connelly, J. N., Amelin, Y., Krot, A. N., & Bizzarro, M. (2008) Chronology of the Solar System's oldest solids. *Astrophysics Journal*, 675, L121–L124.

Connelly, J. N., & Bizzarro, M. (2009) Pb–Pb dating of chondrules from CV chondrites by progressive dissolution. *Chemical Geology*, 259, 143–151.

Connelly, J. N., Bizzarro, M., Krot, A. N., et al. (2012) The absolute chronology and thermal processing of solids in the solar protoplanetary disk. *Science*, 338, 651–655.

Crida, A., Morbidelli, A., & Masset, F. (2006) On the width and shape of gaps in protoplanetary disks. *Icarus*, 181, 587–604.

Dauphas, N., & Chaussidon, M. (2011) A perspective from extinct radionuclides on a young stellar object: The sun and its accretion disk. *Annual Review of Earth and Planetary Sciences*, 39, 351–386.

Dauphas, N., Marty, B., & Reisberg, L. (2002) Molybdenum nucleosynthetic dichotomy revealed in primitive meteorites. *Astrophysics Journal*, 569, L139–L142.

Dauphas, N., & Schauble, E. A. (2016) Mass fractionation laws, mass-independent effects, and isotopic anomalies. *Annual Review of Earth and Planetary Sciences*, 44, 709–783.

Davis, A. M., Zhang, J., Greber, N. D., et al. (2018) Titanium isotopes and rare earth patterns in CAIs: Evidence for thermal processing and gas-dust decoupling in the protoplanetary disk. *Geochimica et Cosmochimica Acta*, 221, 275–295.

Day, J. M. D., & Moynier, F. (2014) Evaporative fractionation of volatile stable isotopes and their bearing on the origin of the Moon. *Philosophical Transactions of the Royal Society A: Mathematical, Physical and Engineering Sciences*, 372, 20130259.

De Sanctis, M. C., Ammannito, E., Capria, M. T., et al. (2012) Spectroscopic characterization of mineralogy and its diversity across Vesta. *Science*, 336, 697.

De Sanctis, M. C., Raponi, A., Ammannito, E., et al. (2016) Bright carbonate deposits as evidence of aqueous alteration on (1) Ceres. *Nature*, 536, 54–57.

Delbo, M., Walsh, K., Bolin, B., Avdellidou, C., & Morbidelli, A. (2017) Identification of a primordial asteroid family constrains the original planetesimal population. *Science*, 357, 1026.

DeMeo, F. E., & Carry, B. (2014) Solar System evolution from compositional mapping of the asteroid belt. *Nature*, 505, 629–634.

Dermott, S. F., Christou, A. A., Li, D., Kehoe Thomas, J. J., & Robinson, J. M. (2018) The common origin of family and non-family asteroids. *Nature Astronomy*, 2, 549–554.

Desch, S. J., Kalyaan, A., & Alexander, C. M. O. (2018) The effect of Jupiter's formation on the distribution of refractory elements and inclusions in meteorites. *Astrophysics Journal Supplementary Series*, 238, 11.

Doyle, P. M., Jogo, K., Nagashima, K., et al. (2015) Early aqueous activity on the ordinary and carbonaceous chondrite parent bodies recorded by fayalite. *Nature Communications*, 6, 7444.

Dwarkadas, V. V., Dauphas, N., Meyer, B., Boyajian, P., & Bojazi, M. (2017) Triggered star formation inside the shell of a Wolf–Rayet bubble as the origin of the Solar System. *Astrophysics Journal*, 851, 147.

Elkins-Tanton, L. T. (2012) Magma oceans in the inner Solar System. *Annual Review of Earth and Planetary Sciences*, 40, 113–139.

Fischer-Gödde, M., Burkhardt, C., Kruijer, T. S., & Kleine, T. (2015) Ru isotope heterogeneity in the solar protoplanetary disk. *Geochimica et Cosmochimica Acta*, 168, 151–171.

Formisano, M., Federico, C., Turrini, D., et al. (2013) The heating history of Vesta and the onset of differentiation. *Meteoritics & Planetary Science*, 48, 2316–2332.

Goldstein, J. I., Scott, E. R. D., & Chabot, N. L. (2009) Iron meteorites: Crystallization, thermal history, parent bodies, and origin. *Geochemistry*, 69, 293–325.

Gradie, J., & Tedesco, E. (1982) Compositional structure of the asteroid belt. *Science*, 216, 1405–1407.

Greenwood, R. C., Burbine, T. H., & Franchi, I. A. (2020) Linking asteroids and meteorites to the primordial planetesimal population. *Geochimica et Cosmochimica Acta*, 277, 377–406.

Heck, P. R., Greer, J., Kööp, L., et al. (2020) Lifetimes of interstellar dust from cosmic ray exposure ages of presolar silicon carbide. *Proceedings of the National Academy of Sciences (USA)*, 117, 1884.

Hellmann, J. L., Kruijer, T. S., Orman, J. A. V., Metzler, K., & Kleine, T. (2019) Hf–W chronology of ordinary chondrites. *Geochimica et Cosmochimica Acta*, 258, 290–309.

Henke, S., Gail, H.-P., Trieloff, M., Schwarz, W. H., & Kleine, T. (2012) Thermal history modelling of the H chondrite parent body. *Astronomy & Astrophysics*, 545, A135.

Hevey, P. J., & Sanders, I. S. (2006) A model for planetesimal meltdown by ^{26}Al and its implications for meteorite parent bodies. *Meteoritics & Planetary Science*, 41, 95–106.

Hilton, C. D., Bermingham, K. R., Walker, R. J., & McCoy, T. J. (2019) Genetics, crystallization sequence, and age of the South Byron Trio iron meteorites: New insights to carbonaceous chondrite (CC) type parent bodies. *Geochimica et Cosmochimica Acta*, 251, 217–228.

Hogerheijde, M. R. (2011) Protoplanetary disk. In M. Gargaud, R. Amils, J. C. Quintanilla, et al. (eds.), *Encyclopedia of Astrobiology*. Berlin: Springer, pp. 1357–1366.

Humayun, M., & Clayton, R. N. (1995) Potassium isotope cosmochemistry: Genetic implications of volatile element depletion. *Geochimica et Cosmochimica Acta*, 59, 2131–2148.

Huss, G. R., & McSween, J. H Y. (eds.) (2010) Presolar grains: A record of stellar nucleosynthesis and processes in interstellar space. In *Cosmochemistry* Cambridge: Cambridge University Press, pp. 120–156.

International Union of Pure and Applied Chemistry (2006) *IUPAC Compendium of Chemical Terminology: The Gold Book*. Research Triangle Park, NC: International Union of Pure and Applied Chemistry.

Ireland, T. R., Avila, J., Greenwood, R. C., Hicks, L. J., & Bridges, J. C. (2020) Oxygen isotopes and sampling of the Solar System. *Space Science Reviews*, 216, 25.

Jacquet, E., Pignatale, F. C., Chaussidon, M., & Charnoz, S. (2019) Fingerprints of the protosolar cloud collapse in the Solar System. II. Nucleosynthetic anomalies in meteorites. *Astrophysics Journal*, 884, 32.

Jaumann, R., Williams, D. A., Buczkowski, D. L., et al. (2012) Vesta's shape and morphology. *Science*, 336, 687.

Jogo, K., Nakamura, T., Ito, M., et al. (2017) Mn–Cr ages and formation conditions of fayalite in CV3 carbonaceous chondrites: Constraints on the accretion ages of chondritic asteroids. *Geochimica et Cosmochimica Acta*, 199, 58–74.

Kita, N. T., & Ushikubo, T. (2012) Evolution of protoplanetary disk inferred from 26Al chronology of individual chondrules: Disk evolution and ^{26}Al chronology of chondrules. *Meteoritics & Planetary Science*, 47, 1108–1119.

Kleine, T., Budde, G., Burkhardt, C., et al. (2020) The non-carbonaceous–carbonaceous meteorite dichotomy. *Space Science Reviews*, 216, 55.

Kleine, T., Hans, U., Irving, A. J., & Bourdon, B. (2012) Chronology of the angrite parent body and implications for core formation in protoplanets. *Geochimica et Cosmochimica Acta*, 84, 186–203.

Kleine, T., Touboul, M., Bourdon, B., et al. (2009) Hf–W chronology of the accretion and early evolution of asteroids and terrestrial planets. *Geochimica et Cosmochimica Acta*, 73, 5150–5188.

Kleine, T., & Wadhwa, M. (2017) Chronology of planetesimal differentiation. In L. T. Elkins-Tanton, & B. P. Weiss (eds.), *Planetesimals: Early Differentiation and Consequences for Planets*. Cambridge: Cambridge University Press, pp. 224–245.

Kleine, T., & Walker, R. J. (2017) Tungsten isotopes in planets. *Annual Review of Earth and Planetary Sciences*, 45, 389–417.

Konopliv, A. S., Park, R. S., Vaughan, A. T., et al. (2018) The Ceres gravity field, spin pole, rotation period and orbit from the Dawn radiometric tracking and optical data. *Icarus*, 299, 411–429.

Krot, A. N., Amelin, Y., Bland, P., et al. (2009) Origin and chronology of chondritic components: A review. *Geochimica et Cosmochimica Acta*, 73, 4963–4997.

Krot, A. N., Keil, K., Scott, E. R. D., Goodrich, C. A., & Weisberg, M. K. (2014) Classification of meteorites and their genetic relationships. In H. D. Holland, & K. K. Turekian (eds.), *Treatise on Geochemistry*. Amsterdam: Elsevier, pp. 1–63.

Krot, A. N., Makide, K., Nagashima, K., et al. (2012) Heterogeneous distribution of ^{26}Al at the birth of the Solar System: Evidence from refractory grains and inclusions: ^{26}Al heterogeneity in the early Solar System. *Meteoritics & Planetary Science*, 47, 1948–1979.

Krot, A. N., Nagashima, K., Libourel, G., & Miller, K. E. (2018) Multiple mechanisms of transient heating events in the protoplanetary disk: Evidence from precursors of chondrules and igneous Ca, Al-rich inclusions. In A. N. Krot, H. C. Connolly Jr., & S. S. Russell (eds.), *Chondrules: Records of Protoplanetary Disk Processes*. Cambridge: Cambridge University Press, pp. 11–56.

Kruijer, T. S., Burkhardt, C., Budde, G., & Kleine, T. (2017) Age of Jupiter inferred from the distinct genetics and formation times of meteorites. *Proceedings of the National Academy of Sciences (USA)*, 114, 6712–6716.

Kruijer, T. S., & Kleine, T. (2019) Age and origin of IIE iron meteorites inferred from Hf-W chronology. *Geochimica et Cosmochima Acta*, 262, 92–103.

Kruijer, T. S., Kleine, T., & Borg, L. E. (2020) The great isotopic dichotomy of the early Solar System. *Nature Astronomy*, 4, 32–40.

Kruijer, T. S., Touboul, M., Fischer-Gödde, M., et al. (2014) Protracted core formation and rapid accretion of protoplanets. *Science*, 344, 1150.

Lambrechts, M., & Johansen, A. (2012) Rapid growth of gas-giant cores by pebble accretion. *Astronomy & Astrophysics*, 544, A32.

Lee, T., Papanastassiou, D. A., & Wasserburg, G. J. (1977) Aluminum-26 in the early Solar System: Fossil or fuel? *Astrophysics Journal*, 211, L107–L110.

Lewis, R. S., Ming, T., Wacker, J. F., Anders, E., & Steel, E. (1987) Interstellar diamonds in meteorites. *Nature*, 326, 160–162.

Leya, I., Schönbächler, M., Wiechert, U., Krähenbühl, U., & Halliday, A. N. (2008) Titanium isotopes and the radial heterogeneity of the Solar System. *Earth and Planetary Science Letters*, 266, 233–244.

Lodders, K. (2003) Solar System abundances and condensation temperatures of the elements. *Astrophysics Journal*, 591, 1220–1247.

Lodders, K., & Amari, S. (2005) Presolar grains from meteorites: Remnants from the early times of the Solar System. *Chemie der Erde – Geochemistry*, 65, 93–166.

Lovering, J. F. (1957) Differentiation in the iron-nickel core of a parent meteorite body. *Geochimica et Cosmochimica Acta*, 12, 238–252.

Lunning, N. G., Corrigan, C. M., McSween, H. Y., et al. (2016) CV and CM chondrite impact melts. *Geochimica et Cosmochimica Acta*, 189, 338–358.

Marchi, S., Raponi, A., Prettyman, T. H., et al. (2019) An aqueously altered carbon-rich Ceres. *Nature Astronomy*, 3, 140–145.

Mayer, B., Wittig, N., Humayun, M., & Leya, I. (2015) Palladium isotopic evidence for nucleosynthetic and cosmogenic isotope anomalies in IVB iron meteorites. *Astrophysics Journal*, 809, 180.

McCord, T. B., Li, J.-Y., Combe, J.-P., et al. (2012) Dark material on Vesta from the infall of carbonaceous volatile-rich material. *Nature*, 491, 83–86.

Morbidelli, A., Bitsch, B., Crida, A., et al. (2016) Fossilized condensation lines in the Solar System protoplanetary disk. *Icarus*, 267, 368–376.

Nagashima, K., Krot, A. N., & Komatsu, M. (2017) ^{26}Al–^{26}Mg systematics in chondrules from Kaba and Yamato 980145 CV3 carbonaceous chondrites. *Geochimica et Cosmochimica Acta*, 201, 303–319.

Nanne, J. A. M., Nimmo, F., Cuzzi, J. N., & Kleine, T. (2019) Origin of the non-carbonaceous–carbonaceous meteorite dichotomy. *Earth and Planetary Science Letters*, 511, 44–54.

Neumann, W., Breuer, D., & Spohn, T. (2014) Differentiation of Vesta: Implications for a shallow magma ocean. *Earth and Planetary Science Letters*, 395, 267–280.

Niemeyer, S. (1988) Titanium isotopic anomalies in chondrules from carbonaceous chondrites. *Geochimica et Cosmochimica Acta*, 52, 309–318.

Ott, U. (2014) Planetary and pre-solar noble gases in meteorites. *Geochemistry*, 74, 519–544.

Papanastassiou, D. A. (1986) Chromium isotopic anomalies in the Allende meteorite *Astrophysics Journal*, 308, L27–L30.

Pape, J., Mezger, K., Bouvier, A.-S., & Baumgartner, L. P. (2019) Time and duration of chondrule formation: Constraints from 26Al–26Mg ages of individual chondrules. *Geochimica et Cosmochimica Acta*, 244, 416–436.

Pollack, J. B., Hubickyj, O., Bodenheimer, P., et al. (1996) Formation of the giant planets by concurrent accretion of solids and gas. *Icarus*, 124, 62–85.

Poole, G. M., Rehkämper, M., Coles, B. J., Goldberg, T., & Smith, C. L. (2017) Nucleosynthetic molybdenum isotope anomalies in iron meteorites – new evidence for thermal processing of solar nebula material. *Earth and Planetary Science Letters*, 473, 215–226.

Prettyman, T. H., Mittlefehldt, D. W., Yamashita, N., et al. (2012) Elemental mapping by Dawn reveals exogenic H in Vesta's regolith. *Science*, 338, 242.

Prettyman, T. H., Yamashita, N., Toplis, M. J., et al. (2017) Extensive water ice within Ceres' aqueously altered regolith: Evidence from nuclear spectroscopy. *Science*, 355, 55.

Qin, L., & Carlson, R. W. (2016) Nucleosynthetic isotope anomalies and their cosmochemical significance. *Geochemical Journal*, 50, 43–65.

Raymond, S. N., & Izidoro, A. (2017a) The empty primordial asteroid belt. *Science Advances*, 3, e1701138.

Raymond, S. N., & Izidoro, A. (2017b) Origin of water in the inner Solar System: Planetesimals scattered inward during Jupiter and Saturn's rapid gas accretion. *Icarus* 297, 134–148.

Reddy, V., Corre, L. L., O'Brien, D. P., et al. (2012) Delivery of dark material to Vesta via carbonaceous chondritic impacts. *Icarus*, 221, 544–559.

Regelous, M., Elliott, T., & Coath, C. D. (2008) Nickel isotope heterogeneity in the early Solar System. *Earth and Planetary Science Letters*, 272, 330–338.

Righter, K. (2007) Not so rare Earth? New developments in understanding the origin of the Earth and Moon. *Geochemistry*, 67, 179–200.

Rotaru, M., Birck, J. L., & Allègre, C. J. (1992) Clues to early Solar System history from chromium isotopes in carbonaceous chondrites. *Nature*, 358, 465–470.

Russell, C. T., Raymond, C. A., Ammannito, E., et al. (2016) Dawn arrives at Ceres: Exploration of a small, volatile-rich world. *Science*, 353, 1008.

Russell, C. T., Raymond, C. A., Coradini, A., et al. (2012) Dawn at Vesta: Testing the protoplanetary paradigm. *Science*, 336, 684.

Sarafian, A. R., Hauri, E. H., McCubbin, F. M., et al. (2017a) Early accretion of water and volatile elements to the inner Solar System: Evidence from angrites. *Philosophical Transactions of the Royal Society A: Mathematical, Physical and Engineering Sciences*, 375, 20160209.

Sarafian, A. R., Nielsen, S. G., Marschall, H. R., et al. (2017b) Angrite meteorites record the onset and flux of water to the inner Solar System. *Geochimica et Cosmochimica Acta*, 212, 156–166.

Sarafian, A. R., Nielsen, S. G., Marschall, H. R., et al. (2019) The water and fluorine content of 4 Vesta. *Geochimica et Cosmochimica Acta*, 266, 568–581.

Sarafian, A. R., Nielsen, S. G., Marschall, H. R., McCubbin, F. M., & Monteleone, B. D. (2014) Early accretion of water in the inner Solar System from a carbonaceous chondrite-like source. *Science*, 346, 623–626.

Schenk, P., O'Brien, D. P., Marchi, S., et al. (2012) The geologically recent giant impact basins at Vesta's south pole. *Science*, 336, 694.

Schiller, M., Bizzarro, M., & Fernandes, V. A. (2018) Isotopic evolution of the protoplanetary disk and the building blocks of Earth and the Moon. *Nature*, 555, 507–510.

Schiller, M., Paton, C., & Bizzarro, M. (2015) Evidence for nucleosynthetic enrichment of the protosolar molecular cloud core by multiple supernova events. *Geochimica et Cosmochimica Acta*, 149, 88–102.

Schrader, D. L., Nagashima, K., Krot, A. N., et al. (2017) Distribution of ^{26}Al in the CR chondrite chondrule-forming region of the protoplanetary disk. *Geochimica et Cosmochimica Acta*, 201, 275–302.

Scott, E. R. D. (1972) Chemical fractionation in iron meteorites and its interpretation. *Geochimica et Cosmochimica Acta*, 36, 1205–1236.

Scott, E. R. D. (1977) Formation of olivine-metal textures in pallasite meteorites. *Geochimica et Cosmochimica Acta*, 41, 693–710.

Scott, E. R. D., Krot, A. N., & Sanders, I. S. (2018) Isotopic dichotomy among meteorites and its bearing on the protoplanetary disk. *Astrophysics Journal*, 854, 164.

Scott, E. R. D., & Wasson, J. T. (1976) Chemical classification of iron meteorites – VIII. Groups IC. IIE, IIIF and 97 other irons. *Geochimica et Cosmochimica Acta*, 40, 103–115.

Shu, F. H., Adams, F. C., & Lizano, S. (1987) Star formation in molecular clouds: Observation and theory. *Annual Review of Astronomy & Astrophysics*, 25, 23–81.

Spitzer, F., Burkhardt, C., Budde, G., et al. (2020) Isotopic evolution of the inner Solar System inferred from molybdenum isotopes in meteorites. *Astrophysics Journal*, 898, L2.

Spitzer, F., Burkhardt, C., Pape, J., & Kleine, T. (in press) Collisional mixing between inner and outer solar system planetesimals inferred from the Nedagolla iron meteorite. *Meteoritics & Planetary Science*.

Sugiura, N., & Fujiya, W. (2014) Correlated accretion ages and ε ^{54} Cr of meteorite parent bodies and the evolution of the solar nebula. *Meteoritics & Planetary Science*, 49, 772–787.

Tang, H., & Dauphas, N. (2012) Abundance, distribution, and origin of 60Fe in the solar protoplanetary disk. *Earth and Planetary Science Letters*, 359–360, 248–263.

Taylor, G. J., Keil, K., McCoy, T., Haack, H., & Scott, E. R. D. (1993) Asteroid differentiation: Pyroclastic volcanism to magma oceans. *Meteoritics*, 28, 34–52.

Tornabene, H. A., Hilton, C. D., Bermingham, K. R., Ash, R. D., & Walker, R. J. (2020) Genetics, age and crystallization history of group IIC iron meteorites. *Geochimica et Cosmochimica Acta*, 288, 36–50.

Touboul, M., Sprung, P., Aciego, S. M., Bourdon, B., & Kleine, T. (2015) Hf–W chronology of the eucrite parent body. *Geochimica et Cosmochimica Acta*, 156, 106–121.

Trinquier, A., Birck, J., & Allegre, C. J. (2007) Widespread ^{54}Cr heterogeneity in the inner Solar System. *Astrophysics Journal*, 655, 1179–1185.

Trinquier, A., Birck, J.-L., Allègre, C. J., Göpel, C., & Ulfbeck, D. (2008) ^{53}Mn–^{53}Cr systematics of the early Solar System revisited. *Geochimica et Cosmochimica Acta*, 72, 5146–5163.

Trinquier, A., Elliott, T., Ulfbeck, D., et al. (2009) Origin of nucleosynthetic isotope heterogeneity in the solar protoplanetary disk. *Science*, 324, 374–376.

Van Kooten, E. M. M. E., Wielandt, D., Schiller, M., et al. (2016) Isotopic evidence for primordial molecular cloud material in metal-rich carbonaceous chondrites. *Proceedings of the National Academy of Sciences (USA)*, 113, 2011–2016.

Vernazza, P., & Beck, P. (2017) Composition of Solar System small bodies. In B. P. Weiss, & L. T. Elkins-Tanton (eds.), *Planetesimals: Early Differentiation and Consequences for Planets*. Cambridge: Cambridge University Press, pp. 269–297.

Villeneuve, J., Chaussidon, M., & Libourel, G. (2009) Homogeneous distribution of 26Al in the Solar System from the Mg isotopic composition of chondrules. *Science*, 325, 985–988.

Vockenhuber, C., Oberli, F., Bichler, M., et al. (2004) New half-life measurement of ^{182}Hf: Improved chronometer for the early Solar System. *Physical Review Letters*, 93, 172501.

Walker, R. J., Bermingham, K., Liu, J., et al. (2015) In search of late-stage planetary building blocks. *Chemical Geology*, 411, 125–142.

Walsh, K. J., Morbidelli, A., Raymond, S. N., O'Brien, D. P., & Mandell, A. M. (2011) A low mass for Mars from Jupiter's early gas-driven migration. *Nature*, 475, 206–209.

Walte, N. P., Solferino, G. F. D., Golabek, G. J., Souza, D. S., & Bouvier, A. (2020) Two-stage formation of pallasites and the evolution of their parent bodies revealed by deformation experiments. *Earth and Planetary Science Letters*, 546, 116419.

Warren, P. H. (2011) Stable-isotopic anomalies and the accretionary assemblage of the Earth and Mars: A subordinate role for carbonaceous chondrites. *Earth and Planetary Science Letters*, 311, 93–100.

Wasson, J. T., & Kallemeyn, G. W. (2002) The IAB iron-meteorite complex: A group, five subgroups, numerous grouplets, closely related, mainly formed by crystal segregation in rapidly cooling melts. *Geochimica et Cosmochimica Acta*, 66, 2445–2473.

Weber, P., Benítez-Llambay, P., Gressel, O., Krapp, L., & Pessah, M. E. (2018) Characterizing the variable dust permeability of planet-induced gaps. *Astrophysics Journal*, 854, 153.

Weidenschilling, S. J. (1977) Aerodynamics of solid bodies in the solar nebula. *Monthly Notices of the Royal Astronomical Society*, 180, 57–70.

Worsham, E. A., Bermingham, K. R., & Walker, R. J. (2017) Characterizing cosmochemical materials with genetic affinities to the Earth: Genetic and chronological diversity within the IAB iron meteorite complex. *Earth and Planetary Science Letters*, 467, 157–166.

Worsham, E. A., Bermingham, K. R., & Walker, R. J. (2016) Siderophile element systematics of IAB complex iron meteorites: New insights into the formation of an enigmatic group. *Geochimica et Cosmochimica Acta*, 188, 261–283.

Worsham, E. A., Burkhardt, C., Budde, G., et al. (2019) Distinct evolution of the carbonaceous and non-carbonaceous reservoirs: Insights from Ru, Mo, and W isotopes. *Earth and Planetary Science Letters*, 521, 103–112.

Yang, J., Goldstein, J. I., & Scott, E. R. D. (2007) Iron meteorite evidence for early formation and catastrophic disruption of protoplanets. *Nature*, 446, 888–891.

Yang, J., Goldstein, J. I., & Scott, E. R. D. (2010) Main-group pallasites: Thermal history, relationship to IIIAB irons, and origin. *Geochimica et Cosmochimica Acta*, 74, 4471–4492.

Yang, L., & Ciesla, F. J. (2012) The effects of disk building on the distributions of refractory materials in the solar nebula. *Meteoritics & Planetary Science*, 47, 99–119.

Yokoyama, T., Nagai, Y., Fukai, R., & Hirata, T. (2019) Origin and evolution of distinct molybdenum isotopic variabilities within carbonaceous and noncarbonaceous reservoirs. *Astrophysics Journal*, 883, 62.

Young, E. D. (2014) Inheritance of solar short- and long-lived radionuclides from molecular clouds and the unexceptional nature of the Solar System. *Earth and Planetary Science Letters*, 392, 16–27.

Zinner, E. (2014) Presolar grains. In A. M. Davis (ed.), *Treatise on Geochemistry*. Amsterdam: Elsevier, pp. 181–213.

Zinner, E., Ming, T., & Anders, E. (1987) Large isotopic anomalies of Si, C, N and noble gases in interstellar silicon carbide from the Murray meteorite. *Nature*, 330, 730–732.